# Barium isotope compositions of altered oceanic crust from the IODP Site 1256 at the East Pacific Rise

Xiao-Yun Nan $^{a,b}$ , Hui-Min Yu $^{a,b,*}$ , Jin-Ting Kang $^{a,b}$ , Fang Huang $^{a,b}$ 

<sup>a</sup>CAS Key Laboratory of Crust-Mantle Materials and Environments, School of Earth and Space Sciences, University of Science and Technology of China, Hefei 230026, China

<sup>b</sup> CAS Center for Excellence in Comparative Planetology, University of Science and Technology of China, Hefei 230026, China

<sup>\*</sup> Correspondences and requests for materials should be addressed to Hui-Min Yu (huy16@ustc.edu.cn).

## Abstract

1

This study reports barium (Ba) isotope compositions of intact altered oceanic crust (AOC) 2 3 recovered from Integrated Ocean Drilling Program (IODP) Site 1256, East Pacific Rise (EPR), to investigate the behavior of Ba isotopes during both low-temperature seawater alteration and 4 high-temperature hydrothermal alteration processes in the oceanic crust. Ba isotope 5 compositions of the volcanic section and sheeted dike complex have large variations and are 6 mostly heavier than the fresh EPR MORB, with  $\delta^{138/134}$ Ba ranging from -0.01% to 0.39%, 7 which may be attributed to the modification of Ba isotopes by seawater and hydrothermal fluid 8 9 during low-temperature and high-temperature alteration. The samples from the plutonic complex display much lighter Ba isotope compositions than the fresh EPR MORB, having 10  $\delta^{138/134}$ Ba values of -0.22% to -0.06%, which may reflect the influence of late magmatic fluids. 11 12 Because of the large Ba isotope variation in the AOC and the obvious difference in Ba isotope compositions between the AOC and the upper mantle, the recycling of the AOC could result in 13 Ba isotope heterogeneity in the mantle and further indicates the application of Ba isotopes for 14 15 tracing crustal material recycling in the Earth's mantle. Keywords: Barium isotopes; Altered oceanic crust; Seawater alteration; Hydrothermal 16 alteration; Crustal material recycling 17

18

19

20

21

22

#### 1. Introduction

Oceanic crust undergoes extensive seawater and hydrothermal alteration before subduction. This process profoundly affects the geochemistry of both seawater and oceanic crust (e.g., Hart et al., 1974; Humphris and Thompson, 1978; Staudigel, 1983; Alt, 1995;

Elderfield and Schultz, 1996; Staudigel, 2014). Clearly, alteration results in significant changes in the chemical (e.g., K and U contents) and isotope compositions (e.g., O, Li, and N isotopes and <sup>87</sup>Sr/<sup>86</sup>Sr) of the oceanic crust (Staudigel et al., 1995; Kelley et al., 2003; Gao et al., 2012; Li et al., 2023). The altered oceanic crust (AOC) is ultimately recycled into the Earth's interior through subduction, thus influencing are volcanism and contributing to the chemical heterogeneities in the mantle (e.g., Hofmann, 1997; Sobolev et al., 2005; Chauvel et al., 2008). Barium (Ba) is highly incompatible during mantle melting and hence is much more enriched in crustal materials than in the mantle (Sun and McDonough, 1989; Plank and Langmuir, 1998; Workman and Hart, 2005; Rudnick and Gao, 2014). Ba is also a fluid-mobile element that could be extracted from the slab during dehydration in subduction (Kessel et al., 2005). Surface reservoirs, such as upper continental materials (e.g., granites, glacial diamictite, loess, and latosol) (Nan et al., 2018; Gong et al., 2019; Deng et al., 2021, 2022; Huang et al., 2021; Jiang et al., 2022), river water (Cao et al., 2016; Gou et al., 2020), groundwater (Mayfield et al., 2021), seawater (Horner et al., 2015; Cao et al., 2016, 2020; Bates et al., 2017; Hsieh and Henderson 2017; Bridgestock et al., 2018; Whitmore et al., 2022), marine sediments (Bridgestock et al., 2018; Nielsen et al., 2020), and AOC (Nielsen et al., 2018), display much larger Ba isotope variations ( $\delta^{138/134}$ Ba of -1.79‰ to +0.95‰) ( $\delta^{138/134}$ Ba =  $[(^{138/134}Ba_{sample})/(^{138/134}Ba_{SRM3104a})-1] \times 1000 \%)$  than the relatively homogeneous upper mantle (average of  $\pm 0.05\%$   $\pm 0.05\%$ , 2SD; Li et al., 2020; Nan et al., 2022; Wu et al., 2023) (summarized in Figure 1). This makes Ba isotopes a potential tracer for crustal material recycling. Recently, Ba isotopes have been used to recognize the contribution of recycled sediments and AOC components in mantle-derived igneous rocks, including mid-ocean ridge

23

24

25

26

27

28

29

30

31

32

33

34

35

36

37

38

39

40

41

42

43

44

basalts (MORB) (Nielsen et al., 2018; Nan et al., 2022; Wu et al., 2023), oceanic island basalts (OIBs) (Bai et al., 2022; Yu et al., 2022a), arc magmas (Nielsen et al., 2020; Wu et al., 2020; Hao et al., 2022), and continental basalts (Zhao et al., 2021; Yi et al., 2022; Shu et al., 2022; Xu et al., 2022). Therefore, knowledge of the Ba isotope compositions of the AOC is essential for identifying the crustal source of the mantle and mantle-derived magmatic systems. To date, only eleven AOC samples from different drilling holes have been reported for Ba isotope compositions, with  $\delta^{138/134}$ Ba ranging from -0.09% to +0.33% (Nielsen et al., 2018). Although large Ba isotope variations in the AOC have been found, little is known about the Ba isotope distribution characteristics and detailed control factors during alteration processes due to the limited Ba isotope data. Consequently, it is critical to study the Ba isotope compositions of an intact alteration profile.

## 2. Geological background and sample descriptions

IODP Site 1256 (6°44.2′N, 91°56.1′W) is located in the Guatemala Basin on the Cocos Plate in the eastern equatorial Pacific Ocean. The drilled oceanic crust was formed ~ 15 Ma ago during an episode of superfast spreading (full rate ~ 220 mm/yr) on the East Pacific Rise (EPR; Wilson 2006). The 1272 m of drilled crustal rocks were recovered at Holes 1256C and 1256D after penetrating ~250 m of sediments (Teagle et al., 2006; Wilson et al., 2003, 2006). Hole 1256C composed of a 32 m thick lava pond is drilled 88.5 m into the basement. Hole 1256D lays ~ 30 m south of 1256C, starting at 276 m below seafloor (mbsf) and extending to a depth of 1507.01 mbsf (Wilson et al., 2006). Based on shipboard core observations and alteration processes (Teagle et al., 2006; Wilson et al., 2006; Alt et al., 2010), Hole 1256D consists of four subdivisions from top to bottom: (i) volcanic section (276.1-1004.2 mbsf); (ii)

lava-dike transition zone (1004.2-1060.9 mbsf); (iii) sheeted dike complex (1060.9-1406.6 mbsf); and (iv) plutonic complex (1406.6-1507.01 mbsf) (Figure 2).

## 3. Analysis methods

The whole-rock powder samples containing 0.5  $\mu g \sim 1~\mu g$  of Ba were weighed into Savillex screw-top Teflon beakers and then digested using a combination of double-subdistilled HF-HNO<sub>3</sub>-HCl. After complete digestion, samples were taken up in 3 mol L<sup>-1</sup> HCl for column separation. Chemical purification of Ba was conducted using chromatographic columns with AG50W-X12 resin (200-400 mesh, Bio-Rad, USA). The sample solution was purified twice using 2 ml AG50W-X12 resin, and Ba was collected using 3 mol L<sup>-1</sup> HNO<sub>3</sub> after eluting the matrix elements using 4 mol L<sup>-1</sup> HCl. An additional column with 0.5 ml AG50W-X12 resin was applied to further separate Ba from rare earth elements (e.g., Ce). Barium was collected in 16 ml of 2 mol L<sup>-1</sup> HNO<sub>3</sub> after matrix elements were eluted with 5 ml of 2 mol L<sup>-1</sup> HNO<sub>3</sub>. The purified sample solutions were dried down and diluted to ~ 100 ng/g with 2% (m/m) HNO<sub>3</sub> for instrumental analyses. The Ba yields of the total purification procedures were >99%. The total procedural blank was <2 ng, which is negligible compared to the Ba amount loaded into the column.

## 4. Results

The Ba isotope data of the samples from IODP Site 1256 are reported in Table 1, along with Ba contents,  $\delta^{18}$ O,  $\delta^{7}$ Li, and Ba/Th ratios previously analysed (Figure 2) (Gao et al., 2012). The  $\delta^{138/134}$ Ba values of seventeen samples from the volcanic section vary from -0.01‰ to 0.39‰ (average of 0.23±0.21‰, 2SD, n=17), exceeding the ranges of fresh EPR N-MORB (-0.04 to

0.08‰, average of 0.05±0.05‰, 2SD; Nielsen et al., 2018; Nan et al., 2022). The  $\delta^{138/134}$ Ba values of the sixteen samples from the transition zone and sheeted dike complex vary from 0.07‰ to 0.38‰, with an average of 0.18±0.18‰ (2SD, n=16). The six samples in the plutonic section have lower  $\delta^{138/134}$ Ba values than the upper sections, ranging from -0.22‰ to -0.06‰ (average of -0.12±0.12‰, 2SD, n=6). The lowermost rock (234R/1) in IODP Site 1256 is a highly altered actinolite-bearing basaltic dike that postdates the intrusion of the lower gabbro (Alt et al., 2010). It has a  $\delta^{138/134}$ Ba value of 0.25‰, existing in the range of the sheeted dike complex and will be discussed as the dike in the following section. The  $\delta^{138/134}$ Ba values of the AOC samples did not correlate with either loss on ignition (LOI) or the chemical index of alteration (CIA) (Figure 3).

## 5. Discussion

The oceanic crust samples at IODP Site 1256 vary from primitive to relatively differentiated compositions with MgO contents ranging from 5.2 wt.% to 10.7 wt.% (Wilson et al., 2006). The  $\delta^{138/134}$ Ba values (-0.22% to 0.39%) vary significantly, with both higher and lower values than that of EPR N-MORB (Figure 2e). This  $\delta^{138/134}$ Ba range is larger than the range of the AOC reported by Nielsen et al. (2018). Such large Ba isotope variation is unlikely inherited from isotope heterogeneity of the pristine oceanic basalts because unaltered MORBs have relatively homogeneous Ba isotope compositions. The variable  $\delta^{138/134}$ Ba values here are most likely produced by Ba isotope fractionation during seawater/hydrothermal alteration at variable temperatures, which is generally accompanied by the dissolution of primary minerals and the formation of secondary minerals.

## 5.1 Ba isotope behaviors during alteration of the volcanic section (276.1-1004.2 mbsf)

The volcanic section at Site 1256 is slightly to moderately altered (2%-20%, Wilson et al., 2006; Alt et al., 2010). Rocks in this section display higher  $\delta^{18}$ O values (6.0% ~ 9.2%) than fresh MORB (5.3% ~ 5.8%, Eiler et al., 2000), indicating seawater alteration at low temperatures (<200°C, Figure 2b; Alt et al., 2010; Gao et al., 2012). The  $\delta^{138/134}$ Ba values of the samples are mostly higher than that of EPR N-MORB and tend toward the values of deep seawater (0.25% ~ 0.45%, Figure 2e) (Horner et al., 2015; Bates et al., 2017; Hsieh and Henderson 2017; Bridgestock et al., 2018), reflecting significant Ba isotope fractionation by low-temperature seawater alteration. However, the  $\delta^{18}$ O and  $\delta^{7}$ Li of whole rocks reflect limited water-rock (w/r) ratios of approximately 2-5 (Gao et al., 2012). The  $\delta^{87}$ Sr/ $\delta^{86}$ Sr (0.70297-0.70327) profile through the volcanic section records minimal Sr isotope exchange from seawater (Harris et al., 2015). There are no clear correlations between  $\delta^{138/134}$ Ba and  $\delta^{18}$ O,  $\delta^{7}$ Li, and  $\delta^{87}$ Sr/ $\delta^{86}$ Sr (Figures 4a, 4b, and 4c), indicating that the Ba isotope distribution signatures in the profile cannot be explained by direct exchange of Ba between fresh MORB and seawater.

As a fluid-mobile element during the alteration of the oceanic crust (Humphris and Thompson,1978), Ba contents in the AOC decreased during primary mineral dissolution and increased by the incorporation/adsorption of Ba-bearing secondary phases. The Ba contents in the altered rocks are thus the net result of these processes. During primary mineral dissolution, Ba isotopes could be fractionated between solution and minerals (Gong et al., 2020). The basalt dissolution experiment at ambient temperature demonstrated that light Ba isotopes are preferentially released from silicate structures into solutions with the  $\Delta^{137/134}$ Ba<sub>fluid-solid</sub> ranging from -0.61‰ to -0.55‰. Based on this result, the heavy Ba isotope compositions observed in

the volcanic section could be caused by losing light Ba isotopes during basalt dissolution with low-temperature seawater alteration.

Overall, we suggest that leaching light Ba isotopes during basalt dissolution during low-temperature alteration is the primary process to produce the observed Ba isotope variation in the volcanic section. Incorporating heavy Ba isotopes from seawater with secondary mineral formation might also increase the  $\delta^{138/134}$ Ba values in the basalts, but it is not the controlling factor.

# **5.2** Ba isotope behaviors during alteration of the transition zone and sheeted dike complex

## (1004.2-1406.6 mbsf)

The transition zone marks the stepwise increase in the alteration temperatures ( $\sim 200^{\circ}\text{C}$ ) and grades with the presence of greenschist facies minerals (Teagle et al., 2006; Alt et al., 2010). The whole-rock  $^{87}\text{Sr}/^{86}\text{Sr}$  compositions reflect the subsurface mixing of seawater and hydrothermal fluids in this section (Harris et al., 2015). Whole-rock  $\delta^{18}\text{O}$  values in the sheeted dikes (3.0%  $\sim 4.8\%$ ) are lower than that of fresh MORB and gradually decrease with increasing depth suggesting a trend of increasing hydrothermal alteration temperature (>250°C, Figure 2b; Gao et al., 2012). The mineral assemblages and strongly elevated  $^{87}\text{Sr}/^{86}\text{Sr}$  ratios (0.704-0.705) indicate pervasive and intensive fluid-rock exchange interactions in the dikes and provide pathways for both seawater-like recharge and upwelling hydrothermal discharge fluids (Teagle et al., 2006; Alt et al., 2010; Harris et al., 2015, 2017).

The  $\delta^{138/134}$ Ba values of basalts in these two sections are variable and fall between those of deep seawater and fresh MORB (Figure 2e). It is noted that global hydrothermal vent fluids are significantly enriched in Ba (1-119  $\mu$ M) relative to seawater (~110 nM) (Tivey, 2007). This is

interpreted to be caused by more Ba being released from rocks to vent fluid at elevated temperatures and pressures because the solubility of Ba is much higher during high-temperature water-rock interactions (Mottl and Holland, 1978; von Damm et al., 1985). Additionally, Hsieh et al. (2021) reported that the  $\delta^{138/134}$ Ba values of endmember hydrothermal vent fluids from mid-oceanic ridge hydrothermal systems are calculated to be between -0.17‰ and +0.09‰, which are comparable to or lower than the  $\delta^{138/134}$ Ba value of fresh MORB. As mentioned in section 5.1, light Ba isotopes are preferentially released to the fluid during low-temperature seawater alteration, and we speculate that lighter Ba leaching from the rocks into the circulating fluids could also be one reason for the heavy Ba isotope signature in the dikes.

Taken together, the  $\delta^{138/134}$ Ba values of the AOC samples are overall higher than that of fresh MORB making it clear that both low-temperature seawater alteration and high-temperature hydrothermal alteration can obviously modify the Ba isotope compositions of oceanic basalts. Their slightly lower Ba/Th ratios than that of fresh MORB reflect the net loss of Ba (Figure 4d). Collectively, it is reasonable to speculate that the heavy Ba isotope characteristics caused by seawater and hydrothermal alteration are mainly attributed to Ba release from the basalts, although the formation of secondary minerals might also play an insignificant role.

## 5.3 Ba isotope behaviors during alteration of the plutonic complex (1406.6-1507.01 mbsf)

The gabbroic rocks in the plutonic section formed through in situ fractional crystallization of a parental MORB melt (Koepke et al., 2011; Teagle et al., 2012). The intrusion of gabbros into the lowermost sheeted dikes resulted in contact metamorphism of the dikes at temperatures of ~800°C–950°C, which produced granoblastic hornfelses in the lower dikes overlying the

gabbros (Koepke et al., 2008; France et al., 2009; Alt et al., 2010; Zhang et al., 2017a). After cooling of the plutonic complex, the gabbros subsequently underwent pervasive hydrothermal alteration under greenschist-facies conditions by the downwards penetration of seawaterderived fluids or upwards magmatic fluids (Teagle et al., 2006; Koepke et al., 2008; Alt et al., 2010). The low porosity granoblastic hornfelses may have served as an impermeable barrier that weakens the fluid fluxes (seawater-derived fluids) penetrating downwards (Alt et al., 2010; Zhang et al., 2017a). The amphiboles in the gabbros are fluorine (F) enriched and formed at 830-910 °C, reflecting reaction with late-stage fluids (Coogan 2001; Koepke et al., 2008; Alt et al., 2010). Because F is moderately incompatible in the mantle and is strongly compatible with hydrous minerals and thus is low in seawater (~1.3 μg/g; Drever, 1997), the F-rich amphiboles should be related to magmatic processes and/or F-rich magmatic fluids (Coogan et al., 2001; Koepke et al., 2008; Kendrick, 2019). A previous study found highly elevated F contents (>1000 µg/g) in the amphiboles analysed in gabbro samples, demonstrating the percolation of F-rich magmatic fluids exsolved from late-stage felsic veins (Kendrick, 2019). In addition, the occurrence of hypersaline inclusions in quartz veins also probably records magmatic fluids (Alt et al., 2010). These lines of evidence strongly point to alteration by the input of magmatic fluids into circulating hydrothermal fluids in the plutonic section.

175

176

177

178

179

180

181

182

183

184

185

186

187

188

189

190

191

192

193

194

195

196

Taken together, the observed light Ba isotope compositions of gabbros in the plutonic section with high Ba/Th may be sourced from late magmatic fluids. The penetration of seawater-derived hydrothermal fluids from the upper layers might also affect the Ba isotopes of gabbros, but magmatic fluid is more likely to dominate the light Ba isotopes in the gabbros. Whatever the origin of the isotopically light Ba in the samples, their existence suggests

differences in alteration conditions with upper layers. Because the Ba isotope fractionation between minerals and fluids remains poorly quantified, more studies are needed to determine the mechanism of Ba isotope fractionation during alteration.

## 6. Conclusions

This study presents a systematic Ba isotope investigation of the AOC profile recovered from IODP Site 1256 in the eastern equatorial Pacific. Their  $\delta^{138/134}$ Ba values vary from -0.22% to 0.39%. Rocks from the volcanic section that experienced low-temperature seawater alteration have higher  $\delta^{138/134}$ Ba (-0.01% to 0.39%) than EPR MORBs and tend to be seawater, suggesting the release of light Ba isotopes from the altered basalt during seawater alteration. Rocks from the transition zone and sheeted dike complex that experienced high-temperature hydrothermal alteration also have higher  $\delta^{138/134}$ Ba values varying from 0.07% to 0.38%, which may be controlled by Ba release from altered basalts during hydrothermal alteration. Rocks from the plutonic complex display lower  $\delta^{138/134}$ Ba than the EPR MORB, which may be induced by the reactions between the late magmatic fluids and gabbros. Our results suggest that subducted AOC and/or sediments could produce varied Ba isotope signatures in the mantle.

## Acknowledgments

We thank Jian Huang, and Ying-Zeng Gong for the discussion. This work is financially supported by the National Natural Science Foundation of China (42073007, 42173003, 42173018).

## References

- Allègre, C.J., Turcotte, D.L., 1986. Implications of a two-component marble-cake mantle.
- Nature 323 (6084), 123-127.
- Alt, J.C., 1995. Subseafloor processes in mid-ocean ridge hydrothermal systems. Washington

- DC, AGU Geophys. Monogr. Ser. 91, 85-114. 220
- Alt, J.C., Laverne, C., Coggon, R.M., Teagle, D.A.H., Banerjee, N.R., Morgan, S., Smith-221
- Duque, C.E., Harris, M., Galli, L., 2010. Subsurface structure of a submarine 222
- hydrothermal system in ocean crust formed at the East Pacific Rise, ODP/IODP Site 1256. 223
- Geochem. Geophys. Geosyst. 11 (10). 224
- Bai, R., Jackson, M.G., Huang, F., Moynier, F., Devos, G., Halldórsson, S.A., Lisiecki, L., Yin, 225
- H., Peng, Y., Nan, X., 2022. Barium isotopes in ocean island basalts as tracers of mantle 226 processes. Geochim. Cosmochim. Acta 336 (1), 436-447. 227
- Bates, S.L., Hendry, K.R., Pryer, H.V., Kinsley, C.W., Pyle, K.M., Woodward, E.M.S., Horner, 228
- T.J., 2017. Barium isotopes reveal role of ocean circulation on barium cycling in the 229
- Atlantic. Geochim. Cosmochim. Acta 204, 286-299. 230
- Bridgestock, L., Hsieh, Y.-T., Porcelli, D., Homoky, W.B., Bryan, A., Henderson, G.M., 2018. 231
- Controls on the barium isotope compositions of marine sediments. Earth Planet. Sci. Lett. 232
- 481, 101-110. 233
- Cao, Z., Siebert, C., Hathorne, E.C., Dai, M., Frank, M., 2016. Constraining the oceanic barium 234
- cycle with stable barium isotopes. Earth Planet. Sci. Lett. 434, 1-9. 235
- 236 Chauvel, C., Lewin, E., Carpentier, M., Arndt, N.T., Marini, J.-C., 2008. Role of recycled
- oceanic basalt and sediment in generating the Hf-Nd mantle array. Nat. Geosci. 1 (1), 64-237 67. 238
- Coogan, L.A., Wilson, R.N., Gillis, K.M., MacLeod, C.J, 2001. Near-solidus evolution of 239
- oceanic gabbros: insights from amphibole geochemistry. Geochim. Cosmochim. Acta 65 240
- (23), 4339-4357. 241
- Deng, G., Jiang, D., Zhang, R., Huang, J., Zhang, X., Huang, F., 2022. Barium isotopes reveal 242
- the role of deep magmatic fluids in magmatic-hydrothermal evolution and tin enrichment 243 in granites. Earth Planet. Sci. Lett. 594, 117724. 244
- Deng, G., Kang, J., Nan, X., Li, Y., Guo, J., Ding, X., Huang, F., 2021. Barium isotope evidence 245
- for crystal-melt separation in granitic magma reservoirs. Geochim. Cosmochim. Acta 292, 246
- 115-129. 247
- 248 Drever, J.I., 1997. The Geochemistry of Natural Waters: Surface and Groundwater
- Environments. Prentice-Hall Inc., Upper Saddle River, New Jersey. 249
- Eiler, J.M., Schiano, P., Kitchen, N., Stolper, E.M., 2000. Oxygen-isotope evidence for recycled 250
- crust in the sources of mid-ocean-ridge basalts. Nature 403 (6769), 530. 251
- Elderfield, H., Schultz, A., 1996. Mid-ocean ridge hydrothermal fluxes and the chemical 252
- composition of the ocean. Annu. Rev. Earth Planet. Sci. 24 (1), 191-224. 253
- France, L., Ildefonse, B., Koepke, J., 2009. Interactions between magma and hydrothermal 254
- system in Oman ophiolite and in IODP Hole 1256D: Fossilization of a dynamic melt lens 255
- at fast spreading ridges. Geochem. Geophys. Geosyst. 10 (10). 256
- Gao, Y., Vils, F., Cooper, K.M., Banerjee, N., Harris, M., Hoefs, J., Teagle, D.A.H., Casey, J.F., 257
- Elliott, T., Laverne, C., Alt, J.C., Muehlenbachs, K., 2012. Downhole variation of lithium 258
- and oxygen isotopic compositions of oceanic crust at East Pacific Rise, ODP Site 1256. 259
- Geochem. Geophys. Geosyst. 13 (10). 260
- Gong, Y., Zeng, Z., Cheng, W., Lu, Y., Zhang, L., Yu, H., Huang, F., 2020. Barium isotopic 261
- fractionation during strong weathering of basalt in a tropical climate. Environ. Int. 143, 262
- 105896. 263

- Gong, Y., Zeng, Z., Zhou, C., Nan, X., Yu, H., Lu, Y., Li, W., Gou, W., Cheng, W., Huang, F., 2019. Barium isotopic fractionation in latosol developed from strongly weathered basalt. Sci. Total Environ. 687, 1295-1304.
- Goss, A., Perfit, M., Ridley, W., Rubin, K., Kamenov, G., Soule, S., Fundis, A., Fornari, D., 2010. Geochemistry of lavas from the 2005–2006 eruption at the East Pacific Rise, 9 46' N–9 56' N: Implications for ridge crest plumbing and decadal changes in magma chamber compositions. Geochem. Geophys. Geosyst. 11 (5).
- Gou, L.-F., Jin, Z., Galy, A., Gong, Y.-Z., Nan, X.-Y., Jin, C., Wang, X.-D., Bouchez, J., Cai, H.-M., Chen, J.-B., 2020. Seasonal riverine barium isotopic variation in the middle Yellow River: Sources and fractionation. Earth Planet. Sci. Lett. 531, 115990.
- Guo, H., Li, W.Y., Nan, X., Huang, F., 2020. Experimental evidence for light Ba isotopes favouring aqueous fluids over silicate melts. Geochem. Perspect. Lett. 16, 6–11.
- Hao, L.-L., Nan, X.-Y., Kerr, A.C., Li, S.-Q., Wu, Y.-B., Wang, H., Huang, F., 2022. Mg-Ba-Sr-Nd isotopic evidence for a mélange origin of early Paleozoic arc magmatism. Earth Planet. Sci. Lett. 577, 117263.
- Harris, M., Coggon, R.M., Smith-Duque, C.E., Cooper, M.J., Milton, J.A., Teagle, D.A.H., 2015. Channelling of hydrothermal fluids during the accretion and evolution of the upper oceanic crust: Sr isotope evidence from ODP Hole 1256D. Earth Planet. Sci. Lett. 416, 56-66.
- Harris, M., Coggon, R.M., Wood, M., Smith-Duque, C.E., Henstock, T.J., Teagle, D.A., 2017.
   Hydrothermal cooling of the ocean crust: Insights from ODP Hole 1256D. Earth Planet.
   Sci. Lett. 462, 110-121.
- Hart, S., Erlank, A., Kable, E., 1974. Sea floor basalt alteration: some chemical and Sr isotopic effects. Contrib. to Mineral. Petrol. 44 (3), 219-230.
- Höfig, T.W., Geldmacher, J., Hoernle, K., Hauff, F., Duggen, S., Garbe-Schönberg, D., 2014. From the lavas to the gabbros: 1.25km of geochemical characterization of upper oceanic crust at ODP/IODP Site 1256, eastern equatorial Pacific. Lithos 210, 289-312.
- Hofmann, A.W., 1997. Mantle geochemistry: the message from oceanic volcanism. Nature 385 (6613), 219.
- Hofmann, A.W., White, W.M., 1982. Mantle plumes from ancient oceanic crust. Earth Planet. Sci. Lett. 57 (2), 421-436.
- Horner, T.J., Kinsley, C.W., Nielsen, S.G., 2015. Barium-isotopic fractionation in seawater mediated by barite cycling and oceanic circulation. Earth Planet. Sci. Lett. 430, 511-522.
- Hsieh, Y.-T., Bridgestock, L., Scheuermann, P.P., Seyfried Jr, W.E., Henderson, G.M., 2021.
  Barium isotopes in mid-ocean ridge hydrothermal vent fluids: A source of isotopically heavy Ba to the ocean. Geochim. Cosmochim. Acta 292, 348-363.

300

## **Figures and Tables**

301

Figure 1. The  $\delta^{138/134}$ Ba values of different geochemical reservoirs, including the AOC at IODP 302 Site 1256 (this study), Holes 504B, 442B, and 417/418 (Nielsen et al., 2018), mantle-303 derived rocks (i.e., MORB, OIB, arc lava, carbonatite, continental basalt, Nielsen et al., 304 2018, 2020; Li et al., 2020; Wu et al., 2020, 2023; Zhao et al., 2021; Bai et al., 2022; 305 Nan et al., 2022; Shu et al., 2022; Xu et al., 2022; Yu et al., 2022a), marine sediments 306 (Bridgestock et al., 2018; Nielsen et al., 2018, 2020), glacial diamictite and loess (Nan 307 et al., 2018), latosol (Gong et al., 2019), and granites (Nan et al., 2018; Deng et al., 308 2021; Huang et al., 2021). The vertical grey bar and blue bar represent the depleted 309 mantle (Nan et al., 2022; Wu et al., 2023) and seawater (Horner et al., 2015; Cao et al., 310 2016; Bates et al., 2017; Hsieh and Henderson 2017; Bridgestock et al., 2018; 311 Whitmore et al., 2022; Yu et al., 2022b), respectively. 312

## 313 Figure 1

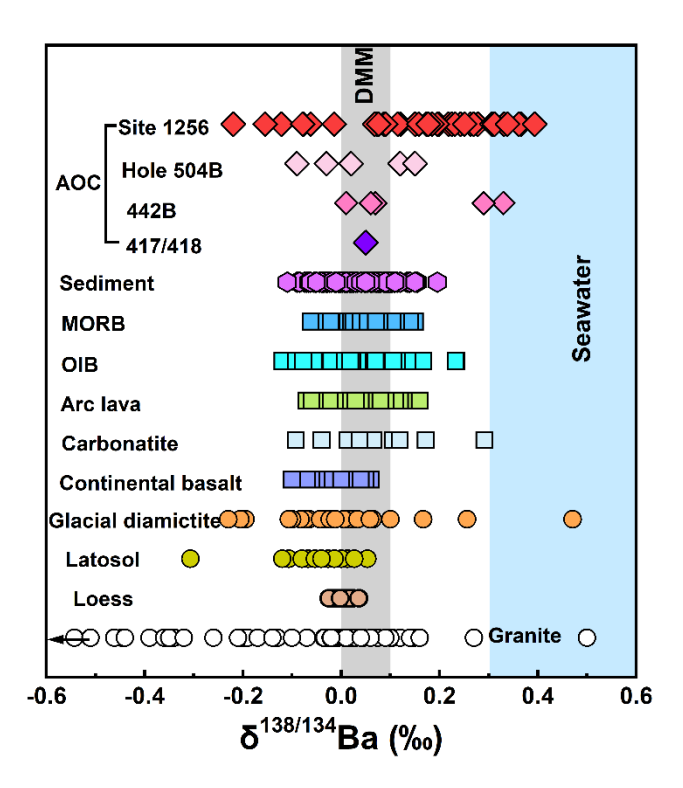


**Table 1** Endmember compositions for the binary mixing model.

	Ba (μg/g)	Sr (µg/g)	<sup>87</sup> Sr/ <sup>86</sup> Sr	δ <sup>138/134</sup> Ba (‰)
DMM	0.563	7.664	0.70219	0.05
AOC-1	22.6	115	0.70458	0.39
AOC-2	22.6	115	0.70458	0.25
AOC-3	22.6	115	0.70458	-0.12
AOC-4	22.6	115	0.70458	-0.22
Sediment-1	786	302	0.7124	0.1
Sediment-2	786	302	0.7124	-0.1

DMM: depleted mantle endmember. Ba and Sr contents and  $^{87}\text{Sr}/^{86}\text{Sr}$  are from Workman and Hart (2005).

The  $\delta^{138/134}$ Ba value is from Nan et al. (2022).

AOC: Ba and Sr contents and  $^{87}$ Sr/ $^{86}$ Sr are from Staudigel et al. (1996). The  $\delta^{138/134}$ Ba values are chosen based on the highest (0.039‰) and lowest values (-0.22‰) of the samples from Site 1256, the average  $\delta^{138/134}$ Ba value for samples from the volcanic section to the sheeted dikes (0.25‰), and the average  $\delta^{138/134}$ Ba value for samples from the plutonic section (-0.12‰).

Sediment: Ba and Sr contents and  $^{87}$ Sr/ $^{86}$ Sr are from Plank (2014). The  $\delta^{138/134}$ Ba values are chosen based on the highest and lowest values of the pelagic sediments reported by Bridgestock et al. (2018) and Nielsen et al. (2018, 2020).